Bulletin of Electrical Engineering and Informatics
Vol. 8, No. 3, September 2019, pp. 818~828
ISSN: 2302-9285, DOI: 10.11591/eei.v8i3.1560

Direct space vector modulation for matrix converter fed dual star induction machine and neuro-fuzzy speed controller

Meliani Bouziane[1], Meroufel Abdelkader[2]
[1]Department of Electrical Engineering, University Centre of Relizane, Algeria
[2]Department of Electrical Engineering, Djillali Liabès University of Sidi Bel-Abbès, Algeria

Article Info

Article history:

Received Jan 9, 2019
Revised Mar 15, 2019
Accepted Apr 5, 2019

Keywords:

Double star
Matrix converter
Neuro-fuzzy
Space vector modulation

ABSTRACT

This paper presents the modeling, design, and simulation of an adaptive neuro fuzzy inference strategy (ANFIS) for controlling the speed of the Double Star induction Machine (DSIM), the machine is fed by three phase direct matrix converter which makes directly AC-AC power conversion is modeled using Direct Space Vector Modulation technique(DSVM) for direct matrix converter. Double star Induction motor is characterized by highly non-linear, complex and time-varying dynamics and inaccessibility of some of the states and outputs for measurements. Hence it can be considered as a challenging engineering problem in the industrial sector. Various advanced control techniques has been devised by various researchers across the world. Some of them are based on the neuro-fuzzy techniques. The main advantage of designing the ANFIS coordination scheme is to control the speed of the DSIM to increase the dynamic performance, to provide good stabilization. To show the effectiveness of our scheme, the proposed method was simulated on an electrical system composed of a 4.5 kW six-phase induction machine and its power inverter. Digital simulation results demonstrate that the deigned ANFIS speed controller realize a good dynamic of the DSIM, a perfect speed tracking with no overshoot, give better performance and high robustness.

Corresponding Author:

Meliani Bouziane,
Department of Electrical Engineering,
University contre of relizane,
Centre Universitaire Ahmed Zabana -Relizane, Bourmadia,
BP 48000, W. Relizane, Algérie.
Email: melianibouziane48@gmail.com

1. INTRODUCTION

The induction motor takes a large place in industry and we can find it in electrical ships. However, when high reliability is required, the control using the field-oriented method is often necessary and on-line diagnosis or off-line diagnoses have to be considered. The use of a double star induction motor or six-phase induction motor is slowly increasing and we find it in the high power process. Its main advantage lies in most reliability in case of a normal operating system [1, 2]. Double star machine supplied with non sinusoidal waveforms causes perturbations in the torque (harmonics in torque). The induction motor drive fed by a matrix converter is superior to the conventional PWM-VS inverter because of the lack of bulky DC-link capacitors with limited life time, the bi-directional power flow capability, the sinusoidal input/output currents, and adjustable input power factor. Various modulation methods for matrix converters have been investigated. Space Vector Modulation (SVM) is one of the preferred modulation methods for three -phase matrix converter [3]. The Space Vector Modulation (SVM) techniques are the extension of the theory of flux in multi-phase rotating machines to the field of static power converters. SVM strategy enables the control of

input power factor independent from output power factor, achieves maximum voltage transfer ratio without the need of third harmonic injection and reduce harmonics [4].

The DSIM it is desirable to control the flux and torque separately in order to have the same performances as those of DC motors. One way of doing this is by using the field oriented control. This method assures the decoupling of flux and torque. The vector-controlled DSIM with a conventional PI speed controller is used extensively in industry, because has easily implemented. Alongside this success, the problem of tuning PI-controllers has remained an active research area. Furthermore, with changes in system dynamics and variations in operating points PI-Controllers should be returned on a regular basis. Today there are many methods for designing intelligent controllers, such as predictive controller, fuzzy control, neural networks and expert systems. Various combinations of these controllers give a number of design possibilities. Artificial Neural Networks (ANNs) and Fuzzy Logic (FL) have been increasingly in use in many engineering fields since their introduction as mathematical aids. A combination of neural networks and fuzzy logic offers the possibility of solving tuning problems and design difficulties of fuzzy logic. The resulting network will be more transparent and can be easily recognized in the form of fuzzy logic control rules or semantics [5]. This new approach combines the well established advantages of both the methods and avoids the drawbacks of both.

2. INDIRECT FIELD ORIENTED CONTROL OF DOUBLE INDUCTION MACHINE

The model of the machine that is established is described by a set of differential equations linking statoric and rotoric magnitudes. The dynamic behavior of this machine supplied by two current inverter is described by a model with rotor flux as state variable [6].

$$\frac{d\varphi_d^r}{dt} = -\frac{1}{T^r}\varphi_d^r + \omega_g\varphi_q^r + \frac{M_c^{sr}}{T^r}(i_{1d}^s + i_{2d}^s) \quad (1)$$

$$\frac{d\varphi_q^r}{dt} = -\frac{1}{T^r}\varphi_q^r + \omega_g\varphi_d^r + \frac{M_c^{sr}}{T^r}(i_{1q}^s + i_{2q}^s) \quad (2)$$

ω_g : being the slip pulsation.

The electromagnetique torque is described by the next equation

$$T_e = \frac{3}{2}p_1\left(\frac{M_c^{sr}}{L_c^r}\right)\left[\varphi_d^r(i_{1q}^s + i_{2q}^s) - \varphi_q^r(i_{1d}^s + i_{2d}^s)\right] \quad (3)$$

P1: number of the pairs vectorial control by orientation of the flux necessitates a choice of judicious referential. The choice of a particular referential allows transforming the expression of the electromagnetic torque so that the induction machine can be compared to D.C machine at least by torque expression. In our study, we have chosen the case of an indirect control by orientation of the rotor flux, whose advantages resides in the simplification and the decoupling of equations of the system. In the model of the double-star asynchronous machine represented by (1) to (3), we choose a referential linked to the rotating field in order that the direct axis D coincides with the desired direction of the rotor flux [7]. This choice of referential imposes $\varphi^r(c) = \varphi_q^r(c) = 0$ and $\varphi_q^r(c) = 0$. Thus (1) to (3) can be written as:

$$T^r\frac{d\varphi_d^t}{dt} + \varphi_d^r = M_c^{sr}(i_{1d}^s + i_{2d}^s) \quad (4)$$

$$\omega_g = \frac{M_c^{sr}}{T^r}\frac{(i_{1q}^s + i_{2q}^s}{\varphi_d^r} \quad (5)$$

$$T_e = \frac{3}{2}p_1\left(\frac{M_c^{sr}}{L_c^t}\right)\varphi_d^r(i_{1q}^s + i_{2q}^s) = \frac{3}{2}p_1\frac{\varphi_d^r}{R^r}\omega_g \quad (6)$$

The mechanical equation is given by:

$$j\frac{d}{dt}\Omega^r + f\Omega^r = T_e - T_c \quad (7)$$

With: T_e : torque of load
j: moment of inertia
f: damping constant of the machine

The model that is established constitutes the main idea of the control of the double star asynchronous machine. We notice that components i_{1d}^{s}andi_{2d}^{s}. If the rotor flux, while the torque depends only of quadrature components of the stator currents i_{1q}^{s}andi_{2q}^{s}. If the rotor flux φ^{r} is maintained constant. For the double star asynchronous machine supplied by current inverter. The stator currents $(i_{1d}^{s}, i_{2d}^{s}, i_{1q}^{s}, i_{2q}^{s})$ and the slip pulsation are considered as variables of control.

3. MATRIX CONVERTER MODELING AND CONTROL

3.1. Modeling for matrix converter

A matrix converter is a variable amplitude and frequency power supply that converts the three phase line voltage directly. It is very simple in structure and has powerful controllability. The real development of the matrix converter starts with the work of Venturini and Alesina who proposed a mathematical analysis and introduced the low frequency modulation matrix concept to describe the low frequency behavior of the matrix converter [8]. In this, the output voltages are obtained by multiplication of the modulation matrix or transfer matrix with the input voltages. The basic diagram of a matrix converter can be represented by Figure 1. The existence function provides a mathematical expression for describing switching patterns. The existence function for a single switch assumes a value of unity when the switch is closed and zero when the switch is open.

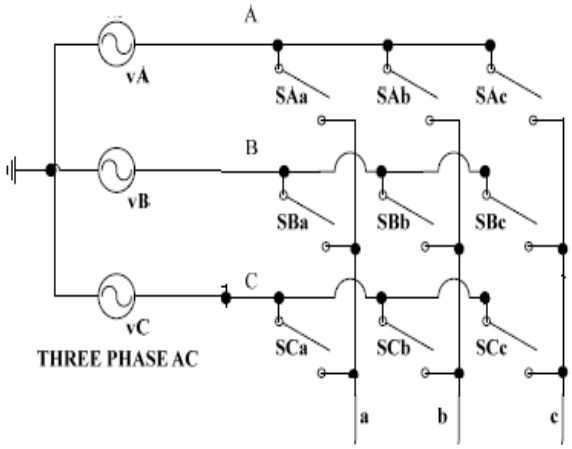

Figure 1. Basic structure of matrix converter

For the matrix converter shown in Figure 2, the existence function for each of the switches is expressed by the following equations:

$$S_{kj} = \begin{cases} 1, \textit{ switch } S_{kj} \textit{ closed} \\ 0, \textit{ switch } S_{kj} \textit{ open} \end{cases} \quad (8)$$

Where k={A, B, C} is input phase and j={a, b, c} is output phase. The above constraint can be expressed in the following form:

$$S_{Aj} + S_{Bj} + S_{Cj} = 1 \quad (9)$$

with the above restrictions a 3x3 matrix converter has 27 possible switching states. The mathematical expression that represents the operation of a three phase ac to ac Matrix Converter can be expressed as follows:

$$\begin{bmatrix} v_a(t) \\ v_b(t) \\ v_c(t) \end{bmatrix} = \begin{bmatrix} S_{Aa}(t) & S_{Ba}(t) & S_{Ca}(t) \\ S_{Ab}(t) & S_{Bb}(t) & S_{Cb}(t) \\ S_{Ac}(t) & S_{Bc}(t) & S_{Cc}(t) \end{bmatrix} * \begin{bmatrix} v_A(t) \\ v_B(t) \\ v_C(t) \end{bmatrix} \quad (10)$$

$$\begin{bmatrix} i_A(t) \\ i_B(t) \\ i_C(t) \end{bmatrix} = \begin{bmatrix} S_{Aa}(t) & S_{Ba}(t) & S_{Ca}(t) \\ S_{Ab}(t) & S_{Bb}(t) & S_{Cb}(t) \\ S_{Ac}(t) & S_{Bc}(t) & S_{Cc}(t) \end{bmatrix}^T * \begin{bmatrix} i_a(t) \\ i_b(t) \\ i_c(t) \end{bmatrix} \quad (11)$$

where va, vb and vc and iA, iB and iC are the output voltages and input currents respectively. To determine the behavior of the MC at output frequencies well below the switching frequency, a modulation duty cycle can be defined for each switch. The modulation duty cycle MKj for the switch SKj in Figure 2 is defined as in (12).

$$M_{kj} = \frac{t_{kj}}{T_s} \quad (12)$$

where tkj is the one time for the switch Skj between input phase k={A, B, C} and j={a, b, c} and Ts is the period of the PWM switching signal or sampling period. In terms of the modulation duty sycle, (13)-(14) can be rewritten as given below.

$$\begin{bmatrix} v_a(t) \\ v_b(t) \\ v_c(t) \end{bmatrix} = \begin{bmatrix} M_{Aa}(t) & M_{Ba}(t) & M_{Ca}(t) \\ M_{Ab}(t) & M_{Bb}(t) & M_{Cb}(t) \\ M_{Ac}(t) & M_{Bc}(t) & M_{Cc}(t) \end{bmatrix} * \begin{bmatrix} v_A(t) \\ v_B(t) \\ v_C(t) \end{bmatrix} \quad (13)$$

$$\begin{bmatrix} i_A(t) \\ i_B(t) \\ i_C(t) \end{bmatrix} = \begin{bmatrix} M_{Aa}(t) & M_{Ba}(t) & M_{Ca}(t) \\ M_{Ab}(t) & M_{Bb}(t) & M_{Cb}(t) \\ M_{Ac}(t) & M_{Bc}(t) & M_{Cc}(t) \end{bmatrix}^T * \begin{bmatrix} i_a(t) \\ i_b(t) \\ i_c(t) \end{bmatrix}$$

$$M_{Aj} + M_{Bj} + M_{Cj} = 1 \quad (14)$$

j={a, b, c}

The high-frequency synthesis technique introduced by Venturini and Alesina in [9, 10] allows the use of low frequency continuous functions, referred to as the modulation matrix m(t), to calculate the existence functions for each switch of the matrix converter. Thus, the aim when using the Alesina and Venturini modulation method is to find a modulation matrix which satisfies the following set of equations.

$$v_o(t) = m(t).v_i(t) \quad (15)$$

$$i_i(t) = m(t)^T.i_o(t) \quad (16)$$

where the input voltages vi(t) are given by the following set of functions

$$v_i(t) = V_{in}\begin{bmatrix} \cos(\omega_i t) \\ \cos(\omega_i t - \frac{2\pi}{3}) \\ \cos(\omega_i t + \frac{2\pi}{3}) \end{bmatrix} \quad (17)$$

and the desired output voltages vo(t) are

$$v_o(t) = V_o\begin{bmatrix} \cos(\omega_o t) \\ \cos(\omega_o t - \frac{2\pi}{3}) \\ \cos(\omega_o t + \frac{2\pi}{3}) \end{bmatrix} \quad (18)$$

output currents $i_o(t)$ can be expressed as:

$$i_o(t) = I_o \begin{bmatrix} \cos(\omega_o t + \varphi_o) \\ \cos(\omega_o t - \frac{2\pi}{3} + \varphi_{\grave{a}}) \\ \cos(\omega_o t + \frac{2\pi}{3} + \varphi_o) \end{bmatrix} \quad (19)$$

Where φ0 is the phase angle of the linear load. Finally, the desired input current has an arbitrary phase φi. This angle can be set to 0 to obtain unity input power factor of the matrix converter.

$$i_i(t) = I_i \begin{bmatrix} \cos(\omega_i t + \varphi_i) \\ \cos(\omega_i t - \frac{2\pi}{3} + \varphi_i) \\ \cos(\omega_i t + \frac{2\pi}{3} + \varphi_i) \end{bmatrix} \quad (20)$$

The elements of matrix m(t) that satisfy (15) and (16) are given by

$$m_{ij}(t) = \frac{1}{3}\alpha\left\{1 + q\cos\left[(\omega_o - \omega_i) + \frac{2}{3}\pi(i-j)\right]\right\} + \frac{1}{3_1}\alpha_2\left\{1 + q\cos\left[(\omega_o - \omega_i) + \frac{2}{3}\pi(2-i-j)\right]\right\} \quad (21)$$

where, $\alpha_1 = \frac{1}{2}\left[1 + \frac{\tan(\varphi_1)}{\tan(\varphi_o)}\right]$, $\alpha_2 = 1 - \alpha_1$, $q = \frac{V_o}{V_i}$

With the following restrictions $\alpha_1 \geq 0$, $\alpha_2 \geq 0$, $0 \leq q \leq \frac{1}{2}$

3.2. Direct space vector modulation technique for matrix converter

The space vector modulation (SVM) is a control technique that has been widely used in adjustable speed drives and more generally in power converter control. The idea of Direct Space Vector Modulation (DSVM) for the matrix converter, unified representation of the current and the voltage space vectors is presented [11]. In an output αβ reference frame, the instantaneous voltage space vector of the output is given by (23). In an input αβ reference frame, the instantaneous current space vector is given by (24).

$$\overline{v_i} = \frac{2}{3}(v_{ab} + \bar{a}\ v_{ab} + \bar{a}^2 v_{ca}) = v_i(t)e^{j\alpha_i(t)} \quad (22)$$

$$\overline{v_o} = \frac{2}{3}(v_{AB} + \bar{a}\ v_{BC} + \bar{a}^2 v_{CA}) = v_o(t)e^{j\alpha_o(t)} \quad (23)$$

$$\overline{i_i} = \frac{2}{3}(i_a + \bar{a}\ i_b + \bar{a}^2 i_c) = i_i(t)e^{j\beta_i(t)} \quad (24)$$

$$\overline{i_o} = \frac{2}{3}(i_A + \bar{a}\ i_B + \bar{a}^2 i_C) = i_o(t)e^{j\beta_o(t)} \quad (25)$$

where vi(t), vo(t) , ii(t) and io(t) are the time dependent magnitudes of the space vectors while αi(t), αo(t), βi(t) and βo(t) are the corresponding time dependent phase angles. For a three phase MC there are 27 valid switch combinations giving thus 27 voltage vectors as shown in Table 1. The switching combinations can be classified into three groups which are, synchronously rotating vectors, stationary vectors and zero vectors.

The DSVM algorithm selects the switching states and calculates the duty cycle for each switching state. During one switching period Ts, the switching states are adjacent to the desired output

voltage (input current) vector, should be selected, and the zero switching states are applied to complete the switching period to provide maximum output to input voltage transfer ratio. Figure 2 shows input and output hexagons, and Table 2 presents the MC states that have to be chosen in terms of reference vectors location.

Table 1. Possible SCS and vectors used in the MC

states	Switches on	$\lvert\vec{v}_o\rvert$	$\langle\vec{v}_o$	$\lvert\vec{i}_o\rvert$	$\langle\vec{i}_o$
ABB +1	S_{Aa} S_{Bb} S_{Bc}	$2/3\ V_{AB}$	0	$2/\sqrt{3}\ i_a$	$-\pi/6$
BAA -1	S_{Ba} S_{Ab} S_{Ac}	$-2/3\ V_{AB}$	0	$-2/\sqrt{3}\ i_a$	$-\pi/6$
BCC +2	S_{Ba} S_{Cb} S_{Cc}	$2/3\ V_{BC}$	0	$2/\sqrt{3}\ i_a$	$\pi/2$
CBB -2	S_{Ca} S_{Bb} S_{Bc}	$-2/3\ V_{BC}$	0	$-2/\sqrt{3}\ i_a$	$\pi/2$
CAA +3	S_{Ca} S_{Ab} S_{Ac}	$2/3\ V_{CA}$	0	$2/\sqrt{3}\ i_a$	$7\pi/6$
ACC -3	S_{Aa} S_{Cb} S_{Cc}	$-2/3\ V_{CA}$	0	$-2/\sqrt{3}\ i_a$	$7\pi/6$
BAB +4	S_{Ba} S_{Ab} S_{Bc}	$2/3\ V_{AB}$	$2\pi/3$	$2/\sqrt{3}\ i_b$	$-\pi/6$
ABA -4	S_{Aa} S_{Bb} S_{Ac}	$-2/3\ V_{AB}$	$2\pi/3$	$-2/\sqrt{3}\ i_b$	$-\pi/6$
CBC +5	S_{Ca} S_{Bb} S_{Cc}	$2/3\ V_{BC}$	$2\pi/3$	$2/\sqrt{3}\ i_b$	$\pi/2$
BCB -5	S_{Ba} S_{Cb} S_{Bc}	$-2/3\ V_{BC}$	$2\pi/3$	$-2/\sqrt{3}\ i_b$	$\pi/2$
ACA +6	S_{Aa} S_{Cb} S_{Ac}	$2/3\ V_{CA}$	$2\pi/3$	$2/\sqrt{3}\ i_b$	$7\pi/6$
CAC -6	S_{Ca} S_{Ab} S_{Cc}	$-2/3\ V_{CA}$	$2\pi/3$	$-2/\sqrt{3}\ i_b$	$7\pi/6$
BBA +7	S_{Bb} S_{Bb} S_{Ac}	$2/3\ V_{AB}$	$4\pi/3$	$2/\sqrt{3}\ i_c$	$-\pi/6$
AAB -7	S_{Aa} S_{Ab} S_{Bc}	$-2/3\ V_{AB}$	$4\pi/3$	$-2/\sqrt{3}\ i_c$	$-\pi/6$
CCB +8	S_{Ca} S_{Cb} S_{Bc}	$2/3\ V_{BC}$	$4\pi/3$	$2/\sqrt{3}\ i_c$	$\pi/2$
BBC -8	S_{Ba} S_{Bb} S_{Cc}	$-2/3\ V_{BC}$	$4\pi/3$	$-2/\sqrt{3}\ i_c$	$\pi/2$
AAC +9	S_{Aa} S_{Ab} S_{Cc}	$2/3\ V_{CA}$	$4\pi/3$	$2/\sqrt{3}\ i_c$	$7\pi/6$
CCA -9	S_{Ca} S_{Cb} S_{Ac}	$-2/3\ V_{CA}$	$4\pi/3$	$-2/\sqrt{3}\ i_c$	$7\pi/6$
AAA O_1	S_{Aa} S_{Ab} S_{Ac}	0		0	
BBB O_2	S_{Ba} S_{Bb} S_{Bc}	0		0	

Table 2. Active vector configurations

		Output voltage reference vector sector											
		1 or 4				2 or 5				3 or 6			
Input current	1 or 4	9	7	3	1	6	4	9	7	3	1	6	4
reference vector	2 or 5	8	9	2	3	5	6	8	9	2	3	5	6
location	3 or 6	7	8	1	2	4	5	7	8	1	2	4	5
		I	II	III	IV	I	II	III	IV	I	II	III	IV

The duty cycle of each selected state id introduced to denote the on-time ratio of that particular switching state during one switching period Ts. δ1, . δ2. δ3 and . δ4 are defined as the duty cycles of the four switching states I, II, III and IV respectively. Kv and Ki denote the sector in which the output voltage and input current space vectors are located in the αβ reference frame. The duty cycles are calculated based on the phase of output voltage and input current vector references such as in the following [12]:

$$\delta_1 = -1^{k_v+k_{i+1}} \frac{2m}{\sqrt{3}} \frac{cos\left(\emptyset'_o-\frac{\pi}{2}\right)cos\left(\emptyset'_i-\frac{\pi}{2}\right)}{cos(\Delta\emptyset)} \quad (26)$$

$$\delta_2 = -1^{k_v+k_{i+1}} \frac{2m}{\sqrt{3}} \frac{cos\left(\emptyset'_o-\frac{\pi}{2}\right)cos\left(\emptyset'_i+\frac{\pi}{6}\right)}{cos(\Delta\emptyset)} \quad (27)$$

$$\delta_3 = -1^{k_v+k_{i+1}} \frac{2m}{\sqrt{3}} \frac{cos\left(\emptyset'_o+\frac{\pi}{6}\right)cos\left(\emptyset'_i-\frac{\pi}{2}\right)}{cos(\Delta\emptyset)} \quad (28)$$

$$\delta_4 = -1^{k_v+k_{i+1}} \frac{2m}{\sqrt{3}} \frac{cos\left(\emptyset'_o+\frac{\pi}{6}\right)cos\left(\emptyset'_i+\frac{\pi}{6}\right)}{cos(\Delta\emptyset)} \quad (29)$$

where m is the modulation index: Δφ is the displacement angle between the measured input voltage vector vi and the input current reference vector ii*, kv and ki are the voltage and current sector, and:

$$\emptyset'_o = \emptyset_o - (k_v - 1)\frac{\pi}{6} \quad (30)$$

$$\emptyset'_i = \emptyset_i - (k_i - 1)\frac{\pi}{6} \quad (31)$$

$$m = \sqrt{3}/2$$

The duty cycles must satisfy (32) in order that the short circuit of any two input phases or open circuit of the load terminals does not occur.

$$|\delta_1| + |\delta_2| + |\delta_3| + |\delta_4| \leq 1 \tag{32}$$

The duty cycle for the zero vector is calculated using (33).

$$\delta_0 = 1 - \{|\delta_1| + |\delta_2| + |\delta_3| + |\delta_4|\} \tag{33}$$

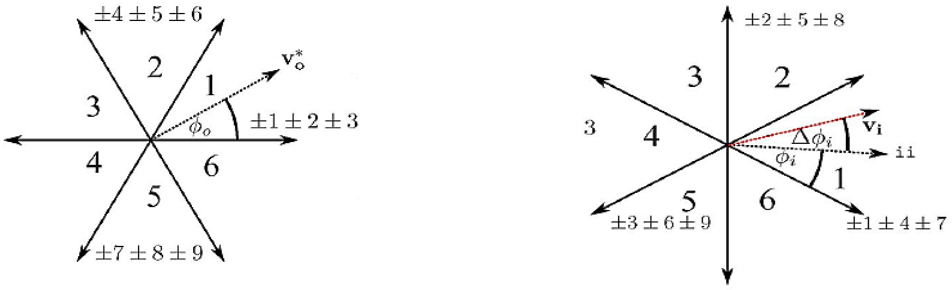

(a) (b)

Figure 2. Available Vectors for SVM, (a) Voltage vectors, (b) Current vectors

4. DESIGN OF ANFIS CONTROLLER

The acronym ANFIS derives its name from adaptive neuro-fuzzy inference system. Using a given input/output data set, the toolbox function anfis constructs a fuzzy inference system (FIS) whose membership function parameters are tuned (adjusted) using either a backpropagation algorithm alone, or in combination with a least squares type of method. This allows your fuzzy systems to learn from the data they are modeling.

ANFIS's network organizes two parts like fuzzy systems. The first part is the antecedent part and the second part is the conclusion part, which are connected to each other by rules in network form. If ANFIS in network structure is shown, that is demonstrated in five layers. It can be described as a multi-layered neural network as shown in Figure 3. Where, the first layer executes a fuzzification process, the second layer executes the fuzzy AND of the antecedent part of the fuzzy rules, the third layer normalizes the membership functions (MFs), the fourth layer executes the consequent part of the fuzzy rules, and finally the last layer computes the output of fuzzy system by summing up the outputs of layer fourth. [13, 14].

In order to model complex nonlinear systems, the ANFIS model carries out input space partitioning that splits the input space into many local regions from which simple local models (linear functions or even adjustable coefficients) are employed. The ANFIS uses fuzzy MFs for splitting each input dimension; the input space is covered by MFs with overlapping that means several local regions can be activated simultaneously by a single input. As simple local models are adopted in ANFIS model, the ANFIS approximation ability will depend on the resolution of the input space partitioning, which is determined by the number of MFs in ANFIS and the number of layers. Usually MFs are used as bell-shaped with maximum equal to 1 and minimum equal to 0, The feed forward equations of ANFIS are as follow [15, 16]:

$$\mu_{Ai}(x) = \frac{1}{1 + [(\frac{x - c_i}{a_i})^2]^{bi}} \tag{34}$$

$$\mu_{Ai}(x) = \exp\left\{-[(\frac{x - c_i}{a_i})^2]^{bi}\right\} \tag{35}$$

Where {ai, bi, ci} are the parameters of MFs which are affected in shape of MFs. In this study the ANFIS controller generates change in the reference voltage V_{ref}, based on speed error e and derivate in the speed error de defined as:

$$e = \omega_{ref} - \omega \quad (36)$$

$$de = [d(\omega_{ref} - \omega)]/dt \quad (37)$$

where ωref and ω are the reference and the actual speeds, respectively. Figure 3 shows the ANFIS model structure.

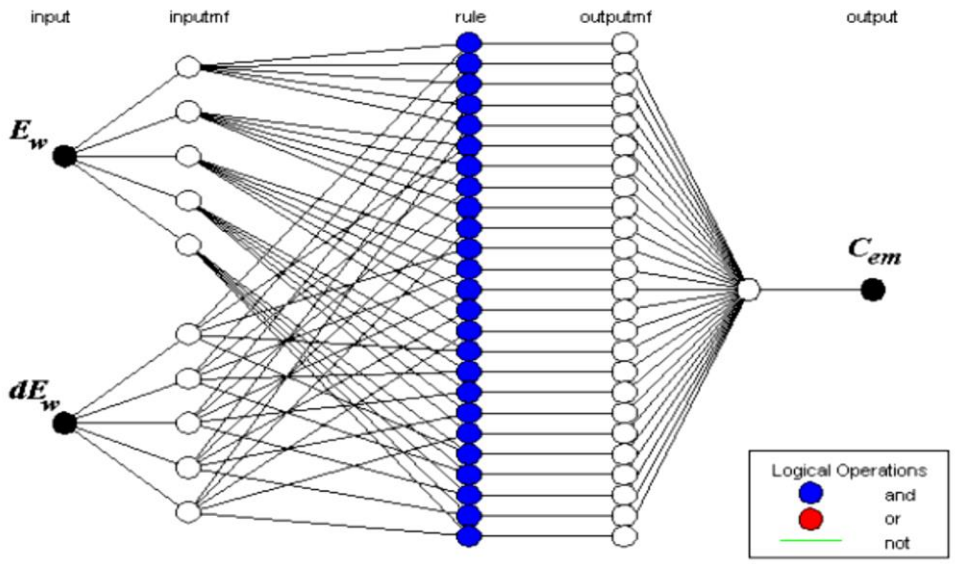

Figure 3. The ANFIS model structure

5. SIMULATION RESULTS

The SIMULINK model for indirect FOC of the 4.5 Kw cage rotor DSIM associated with ANFIS controller is shown in Figure 4. The machine is fed by a matrix converter with Space vector modulation Technique. The parameters of the induction motor are summarized in Appendix. The first test concerns a no-load starting of the motor with a reference speed ω_{ref} = 288 rad/sec. and a nominal load disturbance torque (14N.m) is suddenly applied between 1sec and 2sec, followed by a consign inversion (-288rad/sec) at 2.5sec. At 4.5s, a -14Nm load disturbance is applied during a period of 2 s. this test has for object the study of controller behaviors in pursuit and in regulation. The test results obtained are shown in Figure 5.

The speed of the motor reaches ω_{ref} at 0.2 s with almost no overshoot. It then begins to oscillate inside a 0.4% error strip around ω_{ref} . The ANFIS controller rejects the load disturbance very quickly with no overshoot and with a negligible steady state error. In order to test the robustness of the used method we have studied the effect of the parameters uncertainties on the performances of the speed control. To show the effect of the parameters uncertainties, we have simulated the system with different values of the parameter considered and compared to nominal value (real value). The Figure 6 and Figure 7 show respectively the behavior of the DSIM when Rr is 10% increased of its nominal value and J is increased 10% of its nominal value. An increase of the moment of inertia gives best performances, but it presents a slow dynamic response. The figures show that the proposed controller gave satisfactory performances thus judges that the controller is robust.

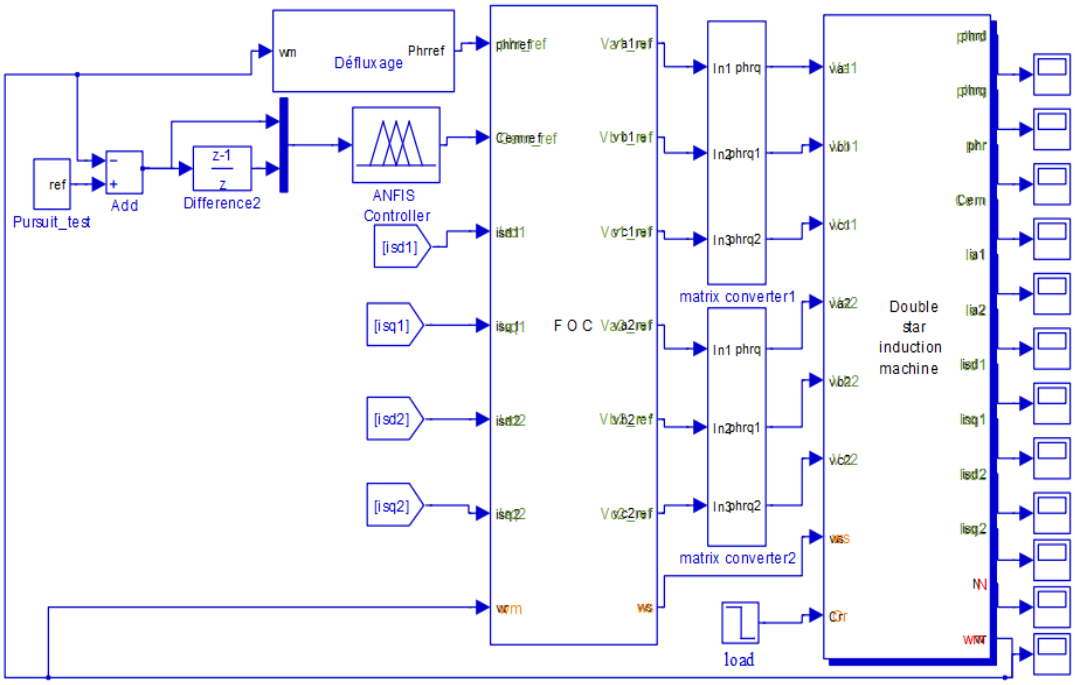

Figure 4. Simulink diagram for DSIM control systems

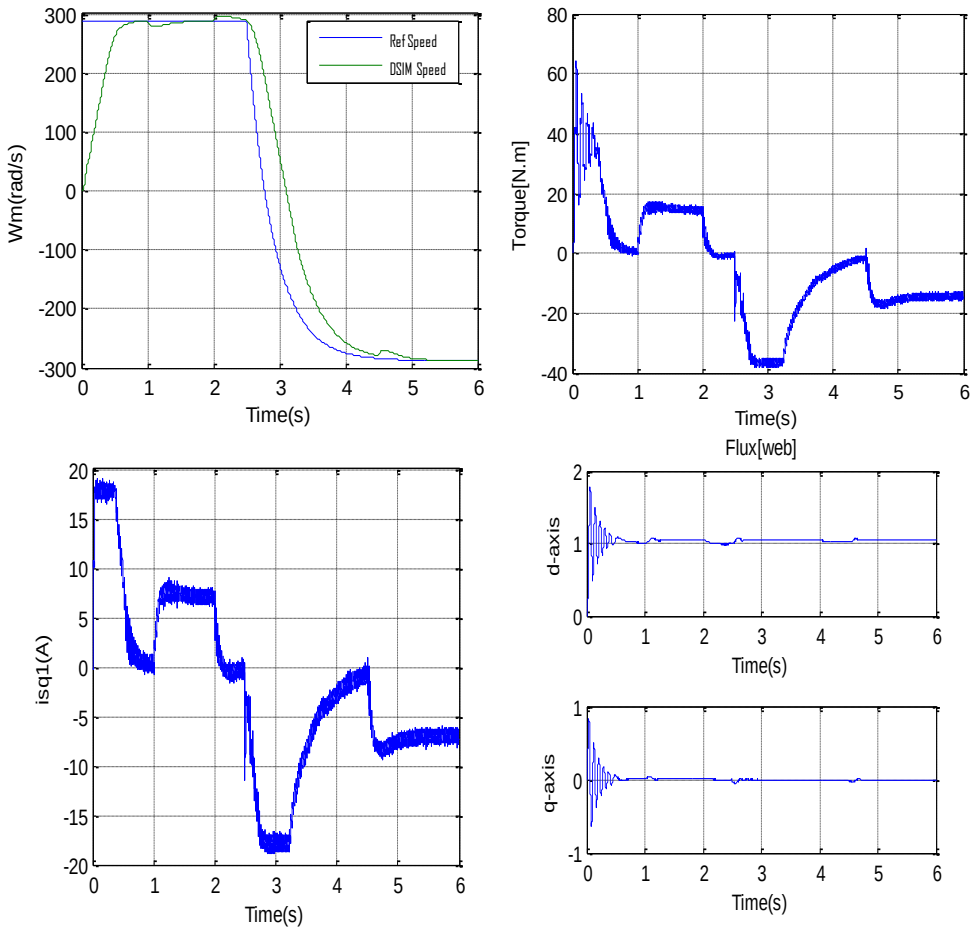

Figure 5. Simulated results of ANFIS controller for DSIM

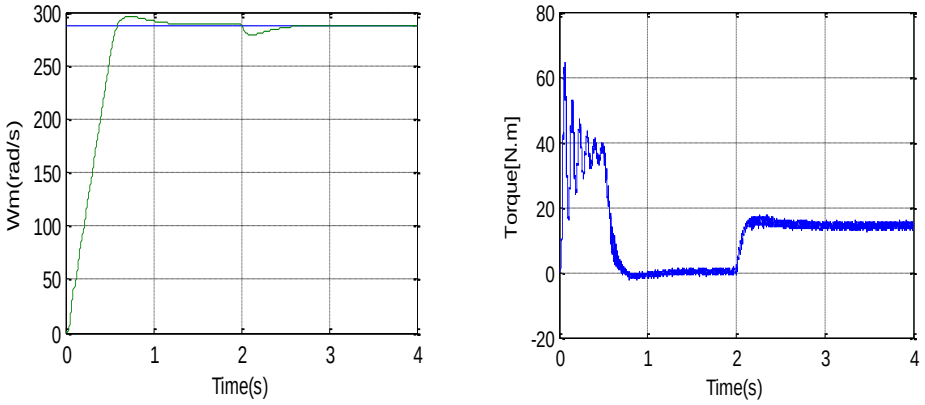

Figure 6. Simulated results of ANFIS controller for DSIM with variation of the rotor inertia (+10%J)

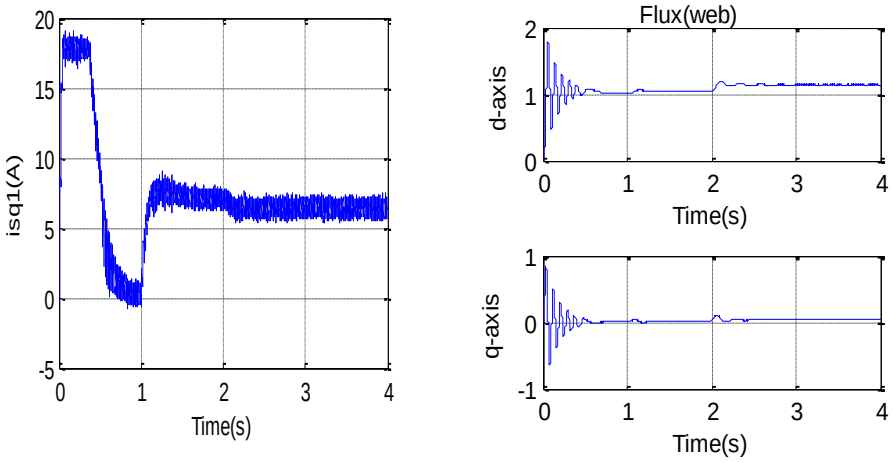

Figure 7. Simulated results of ANFIS controller for DSIM with variation of the rotor resistance at t=2s

6. CNCLUSION

This paper presents a study of an application of speed control with neuro fuzzy inference strategy (ANFIS) controller for a double stator induction machine based on the direct FOC, The machine is fed by a matrix converter, Simulation results on control robustness with speed variation parameters variation and the torque resistant are given. The results show that the controller could compensate for this kind of disturbances. The plant is also tested for the tracking property using different types of reference signals. Satisfactory performance was observed for most reference tracks and the results demonstrated the effectiveness of the proposed structure and the proposed control scheme it is believed will constitute a major step in the evolution of intelligent control

REFERENCES

[1] A.S.O.OgunjuyigbeT.R.AyodeleB.B.Adetokun "Modelling and analysis of dual stator-winding induction machine using complex vector approach" *Engineering Science and Technology, an International Journal*,Volume 21, Issue 3, June 2018, Pages 351-363

[2] Basak, S., Chakraborty, C " Dual stator winding induction machine: Problems, progress, and future scope" *IEEE Transactions on Industrial Electronics,* Volume 62, Issue 7, 1 July 2015, Pages 4641-4652

[3] D.Sri Vidhya, T. Venkatesan "A Review on Performance Analysis of Matrix converter Fed AC Motor Drive" *International Journal of Electrical and Drive System*, Vol. 7, No.1, March 2016,PP.85-93

[4] Gang Li "Realization of SVM Algorithm for Indirect Matrix Converter and Its Application in Power Factor Control", *Advances in Power Electronics* Volume 2015, Article ID 740470, 10 pages
[5] Larafi Bentouhamia, Rachid Abdessemedb, Abdelhalim Kessala, Elkhier Merabeta, "Control Neuro-Fuzzy of a Dual Star Induction Machine (DSIM) supplied by Five-Level Inverte r", *Journal of Power Technologies* 98 (1) (2018) 70–79
[6] D. Hadiouche, "Contribution to the study of dual stator induction machines: modelling, supplying and structure", Ph. D. dissertation (in french), GREEN, Faculty of Sciences and Techniques, University Henri Poincaré-Nancy I, France, Dec. 2001.
[7] Bojoi R., Tenconi A., Griva G., Profumo F, "Vector Control of Dual-Three-Phase induction-Motor Drives Using Two Current Sensors ", *IEEE Trans. on Industry Applications*, vol. 42, no. 5, pp. 1284-1292, September/October 2006.
[8] M. Venturini and A. Alesina, "Generalised transformer: A new Bidirectional, Sinusoidal Waveform Frequency Converter with Continuously Adjustable Input Power Factor," PESC Rec *IEEE Power Electronics Specialists Conference, Atlanta*, USA, 1980, pp. 242-252.
[9] Jose Rodriguez , Marco Rivera, Johan W. Kolar, and Patrick W. Wheeler , " A Review of Control and Modulation Methods for Matrix Converters " *IEEE Transactions On Industrial Electronics*, Vol. 59, No. 1, January 2012
[10] J. Vadillo ; J. M. Echeverria ; A. Galarza ; L. Fontan, " Modelling and Simulation of Space Vector Modulation Techniques for Matrix Converters: Analysis of different Switching Strategies " *ICEMS 2008. International Conference on Electrical Machines and Systems*
[11] M. Rameshkumar, Y. Sreenivasa Rao and A. Jaya laxmi , "Modulation And Control Techniques Of Matrix Converter" *International Journal of Advances in Engineering & Technology*, July 2012..
[12] M. Jussila and H. Tuusa, "Comparison of simple control strategies of space-vector modulated indirect matrix converter under distorted supply voltage," *IEEE Transactions on Power Electronics*, vol. 22, no. 1, pp. 139–148, 2007.
[13] Jyh-Shing Roger Jang, " ANFIS : Adaptive-Network Based Fuzzy Inference System ", *IEEE Transactions on systems, Man, And Cybernetics*, Vol, 23, No,3, May/june 1993
[14] V. Chitra, "ANFIS Based Field Oriented Control for Matrix Converter fed Induction Motor", *IEEE international conference on power and energy* (PECon2010), Malaysia, 7478
[15] Hechelef Mohammed, Abdelkader Meroufel, Omar .Ouledali, "Contribution to the Artificial Neural Network Direct Control of Torque Application Utilizing Double Stars Induction Motor", *Australian Journal of Basic and Applied Sciences*, 335-342, January,2014
[16] S.R. Khuntia, K.B. Mohanty, S. Panda and C. Ardil , "A Comparative Study of P-I, I-P, Fuzzy and Neuro-Fuzzy Controllers for Speed Control of DC Motor Drive" *International Journal of Electrical and Computer Engineering* 5:5 2010

APPENDIX

Table 3. DSIM parameters

N nominal values	Value	IS-Unit
Power	4.5	kW
Frequency	50	Hz
Voltage (Δ /Y)	220/380	V
Current (Δ /Y)	5.6	A
Speed	2751	rpm
Constant	Value	IS-Unit
Poles of pair	1	
$Rs_1 = Rs_2$	3.72	Ω
Rr	2.12	Ω
$Ls_1 = Ls_2$	0.022	H
Lr	0.006	H
L_m	0.3672	H
J	0.0625	Kgm^2
K_f	0.001	$Nm(rad/s)^{-1}$